

# Improvement of Sliding Property and Other Performance in Chromium Free Hot Dip Galvanizing Steel Sheet “DURGRIP™ QS2”

Ken TOMIYASU\*  
Yasuo TSUJIMOTO

Hiroki TAKAMARU  
Eiji MAEDA

## Abstract

**DURGRIP™ QS2 is a chromium free hot dip galvanized steel sheet which gives the compatibility to a various sheet metal processing processes carried out in a steel sheet user. The compatibility depends on the design of the surface thin film layer. Almost of conventional film layers have been containing lubricant to adapt to non-oiling press forming. However, the badness of the handling such as a coil collapse or sheet pile break by the slip, as the side effect of increased lubricity, is a serious problem. In this paper, the balance advancement between the press formability and compatibility to handling has been examined, and the effect of these examinations was inspected. In addition, other compatibilitys mentioned above were confirmed enough at the same time.**

## 1. Introduction

In recent days, reduction of material cost of home electric appliances has grown to be a matter of serious issue due to aggravation of price competition. Therefore, cases of switching to hot dip galvanized steel sheet from pre-coated steel sheet (PCM) and electro-galvanized steel sheet is increasing. The reasons for selecting hot dip galvanized steel sheet as the alternate material are as follows: ① home electric appliance design and practical requirement for surface quality, ② low cost, ③ worldwide production and convenience of procurement. In contrast, demand for higher surface quality of hot dip galvanized steel sheet and improvement in compatibility to home electric appliance production processes are continuously growing.

DURGRIP™ QS2 is a hot dip galvanized steel sheet with enhanced universality, provided with adaptability to sheet-forming processes in wide range conducted in steel sheet users, characterized by chromium-free-treated coating film of organic and non-organic system as shown in Fig. 1 which provides; ① corrosion resistance sufficient to eliminate rust-preventing painting, ② lubricity sufficient to enable non-oiling press forming, thereby eliminating degreasing process, ③ resistance welding weldability like spot welding, and ④ adhesion property of overcoat painting in case of painting.

Lubricity is provided by the coating film layer containing solid lubricant on the galvanized steel sheet surface. The background that accounts for the regulation of Freon gas enforced in 1995, restricts the use of solvent of the Freon system which had been widely and popu-

larly used as the degreasing and cleaning agent, and the subject coating is based on the concept of eliminating the degreasing process itself corresponding to the employment of non-oiling press forming as a countermeasure to the above. In contrast, troubles in handling coils such as coil collapses and coil pile breaks took place on account of lubricity provided. Photo 1 shows an example where the coiling of a

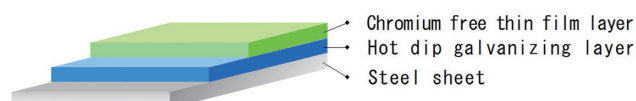


Fig. 1 Film composition of DURGRIP™ QS2 (front and back of the sheet are same)



Photo 1 Coil collapse accident example

\* Senior Manager, Steel Sheet Products Development Dept., Quality Management Div., Kashima Works  
3 Hikari, Kashima City, Ibaraki Pref. 314-0014

sheet coil became loose during land transportation and the strapping bands were broken right after arrival, and the situation almost came near to a disastrous reality.

In the development of DURGRIP™QS2, particularly the improvement in the compromise between lubricity and problems in handling, a side effect of lubricity, was studied. Furthermore, compatibility of other performances as mentioned above was also confirmed.

## 2. Experiment

### 2.1 Coating treatment

The coating film layer is formed by roller coating onto a steel sheet a liquid containing the coating film compositions and then drying it. It is indicated that many of the solid lubricants are enriched on the coating film surface after roller coating and drying since such lubricants contained in the liquid have a surface tension lower than those of any solvents and other coating film compositions in addition to water.<sup>1)</sup> When the solid lubricant is dispersed in the coating film layer to eliminate the enriching on the coating film surface, it is expected that under the high contact pressure sliding condition in press forming, the solid lubricant in the coating film layer functions as the coating film layer is deformed and flows. On the other hand, under the low contact pressure in coils in the state of stillness similar to coil handling and piled-sheet handling, the coating film layer is not deformed and does not flow. Therefore, the solid lubricant in the coating film layer does not function.<sup>2)</sup> Thus, to disperse the solid lubricant in the coating film, a method was studied to disperse it in the coating film by enhancing the surface energy of the solid lubricant by chemically modifying the lubricant surface. **Photo 2** shows the secondary electron (SE) image of an example of the coating film layer added with surface-modified solid lubricant. **Photo 3** shows the SE image of an example of the coating film layer added with solid lubricant without modified surface. The surface-modified solid lubricant is soaked in the coating film layer, whereas the solid lubricant without surface modification is seen exposed on the surface.

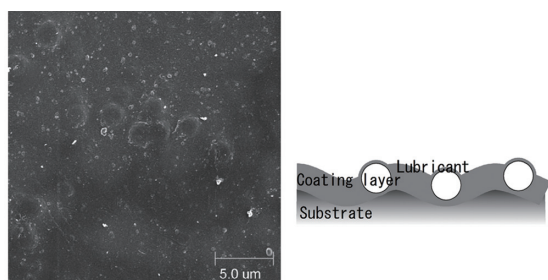


**Photo 2** SE image of the film layer surface and section illustration  
Example which added solid lubricant with surface modify

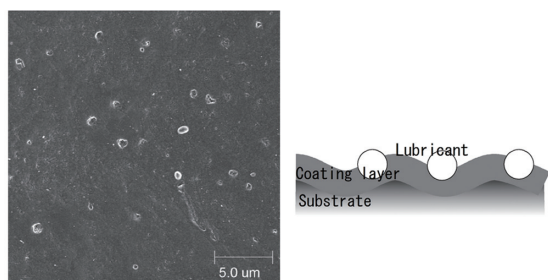


**Photo 3** SE image of the film layer surface and section illustration  
Example which added solid lubricant without surface modify

### 2.2 Evaluation of press formability

#### 2.2.1 Method of evaluating press formability

Following coating films were catered for evaluation: coating film added with surface-modified solid lubricant (A), coating film added with solid lubricant without surface-modification (B), coating film without lubricant for comparison purpose (C), and coating film sample (C) coated with anti-rust forming oil for further comparison (D). Detailed specifications of the coating film samples are shown in **Table 1**. As any of A, B, C, and D are mass-produced materials and widely available in market, their data are limited to the minimum required for the understanding of the phenomena, and therefore, standards are not shown. A is DURGRIP™QS2.

Cylinder drawing was conducted for press forming test. Press forming test was conducted at each 15 kN increment of the flange blank holding force ( $F_{BH}$ ) and terminated when the material fracture took place. **Table 2** shows the detail of the mechanical condition.

Press forming under the standard lubrication condition was also conducted to establish lubrication performance evaluating standard. Standard lubrication condition is the state of the blank being protected on both sides by polyester sealing tapes and coated with high viscosity press forming oil. The relationship between the forming load ( $F_p$ ) and the blank holding load  $F_{BH}$  in the standard lubrication condition is shown in **Fig. 2**. Since a constant value of  $F_p$  was observed regardless of  $F_{BH}$ ,  $F_p$  under the standard lubrication condition may be considered as the net forming force which does not include the contribution of frictional force.

Using the values of  $F_p$ ,  $F_{BH}$  and the punch stroke ( $s_p$ ) corresponding to  $F_p$ , and the forming load under the standard lubrication condition  $F_p^*$ , calculation of coefficient of friction was attempted. Assuming that the forming tension ( $T$ ) shown in **Fig. 3** is the sum of the net forming load ( $T^*$ ) and the blank holder frictional force ( $\mu F_{BH}$ ), a model formula with respect to  $T$  where the blank undergoes drawing at a winding angle of ( $\phi$ ) at the die shoulder is shown as formula (1).

$$T = F_p / \sin \phi^{app} = (T^* + \mu F_{BH}) e^{\mu \phi} \div (T^* + \mu F_{BH}) (1 + \mu \phi) \quad (1)$$

**Table 1** Details of test materials

Coating	Lubricant (included in coating)	Plating layer (finish of substrate)	Sheet thickness mm	Steel class
A	Modified solid lubricant	Hot-dip galvanizing	0.6	Low carbon steel
B	Conventional solid lubricant	Hot-dip galvanizing	0.6	Low carbon steel
C	Not added	Hot-dip galvanizing	0.6	Low carbon steel
D	Coating C and anti-rust forming oil	Hot-dip galvanizing	0.6	Low carbon steel

**Table 2** Press forming condition of cylinder drawing

Condition item	Details of condition
Punch specifications	Punch outer diameter: 50 mm, Radius of punch shoulder curvature R: 5 mm
Dice specifications	Dice inside diameter: 52 mm, Radius of dice shoulder curvature R: 5 mm
Forming condition	Diameter of steel sheet blank: 90 mm (drawing ratio: 1.8) Rate of forming: 200 mm · min <sup>-1</sup> , Blank hold load: 15 - 150 kN

The winding angle of ( $\phi^{app}$ ) is obtained with the formula (2) led from the geometric condition that the inner product of the contact point vector and the common tangent vector is zero (Fig. 4). However, since the actual winding angle is affected by the rigidity of the material, formula (3) is used for compensation. From the above, the coefficient of friction ( $\mu$ ) is led by formula (4).

$$\phi^{app} = \arcsin \left( \frac{2(R+t/2)(g+2R) + (s_p - 2R) \{ (s_p - 2R)^2 + (g+2R)^2 - 4(R+t/2)^2 \}^{1/2}}{(g+2R)^2 + (s_p - 2R)^2} \right) \quad (2)$$

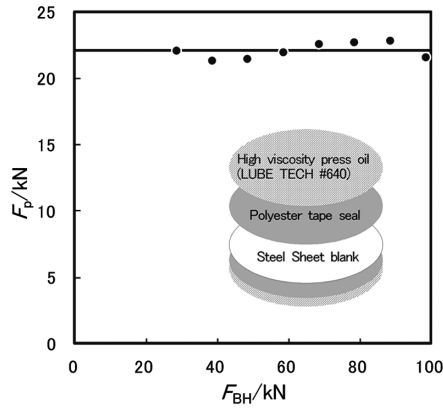


Fig. 2 Relations with forming load ( $F_p$ ) and the blank holding load ( $F_{BH}$ ) in the comparison lubrication condition

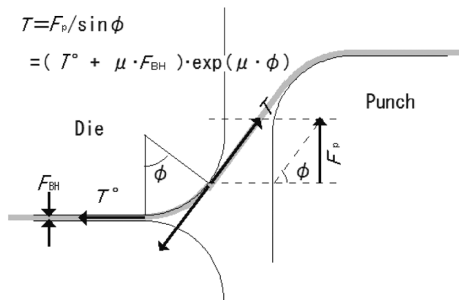


Fig. 3 Forming tension model to separate a pure forming load and pure friction, and to reconstitute them

$$\phi = \phi^{app} \cdot \exp \{ -0.10 \cdot T^\circ / (T - T^\circ) \} \quad (3)$$

$$\mu = \frac{-\phi T^\circ - F_{BH} + \{ (\phi T^\circ + F_{BH})^2 - 4\phi F_{BH} (T^\circ - T) \}^{1/2}}{2\phi F_{BH}} \quad (4)$$

where  $\mu$ : coefficient of friction,  $F_p$ : forming load,  $T$ : forming tension,  $T^\circ$ : net forming tension,  $\phi^{app}$ : appearing die shoulder winding angle,  $\phi$ : die shoulder winding angle,  $s_p$ : punch stroke at maximum forming load,  $R$ : radius of curvature of die shoulder = radius of curvature of punch shoulder,  $g$ : (die diameter-punch diameter)/2,  $t$ : blank sheet thickness.

#### 2.2.2 Result of evaluation of press formability

Table 3 shows the result obtained. Figure 5 shows the relationship between the coefficient of friction and the blank holding condition (blank holding force/net forming tension). A and B show nearly equal low coefficients of friction and the blanks could be formed in the range wider than that of D coated with anti-rust forming oil. This fact means that the coating films of A and B are excellent as lubricant. For C not provided with lubricity, there was a tendency of coefficient of friction rising as the blank holding force going higher. Photo 4 shows the appearance of the test sample after 48 h in salt spray test (SST) after the cylindrical forming. Although A is excellent, a trend is observed that the higher the coefficient of friction becomes, the more noticeable the white rust appearing in the sphere ranging from the flange to the vertical wall becomes, wherein the flange is subject to very severe sliding condition caused by severe deformation.

From the above, it is found that press formability is excellent re-

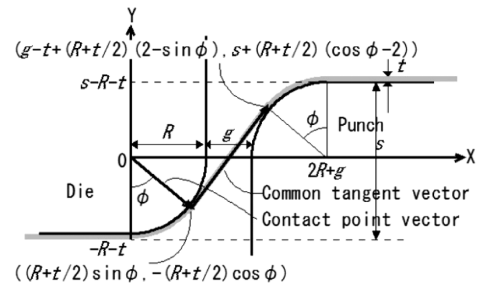


Fig. 4 Geometric condition to decide the winding angle to dice shoulder

Table 3 Result of press forming and calculation result of the frictional coefficient

Coating	Examined lubrication condition					Comparison lubrication condition					Result of calculations					
	$F_{BH}$ kN	$F_p$ kN	$s_p$ mm	$\phi^{app}$ rad	Forming	$F_{BH}^\circ$ kN	$F_p^\circ$ kN	$s_p^\circ$ mm	$\phi^{app}$ rad	Forming	$T_p$ kN	$T_p^\circ$ kN	$T_p^\circ$ $T_p - T_p^\circ$	$\phi$ rad	$F_{BH}$ $T_p^\circ$	$\mu$ Mean $\pm 1\sigma$
A	30.0	29.4	15.8	1.47	OK	60.0	23.48	15.5	1.46	OK	29.6	24.0	4.4	0.94	1.2	0.124
A	45.0	32.6	16.9	1.48	OK	60.0	24.0	15.5	1.5	OK	32.7	24.0	2.8	1.11	1.9	0.132
A	60.0	34.2	16.6	1.48	OK						34.4	24.0	2.3	1.2	2.5	0.125
A	75.0	36.8	17.0	1.48	OK						36.9	24.0	1.9	1.2	3.1	0.127
A	90.0	38.2	13.8	1.42	Break						38.6	24.3	1.7	1.3	3.7	0.124
B	45.0	30.3	15.4	1.46	OK	60.0	24.0	15.5	1.5	OK	30.5	24.0	3.7	0.99	1.9	0.111
B	60.0	32.2	14.9	1.45	OK	60.0	23.8	15.5	1.46	OK	32.5	24.0	2.8	1.1	2.5	0.111
B	75.0	35.8	15.5	1.46	OK						36.1	24.0	2.0	1.2	3.1	0.123
B	90.0	37.4	17.0	1.48	Break						37.8	24.0	1.8	1.2	3.7	0.119
C	15.0	29.1	17.2	1.48	Crease	60.0	24.3	15.5	1.46	OK	29.2	24.0	4.6	0.92	0.6	0.158
C	30.0	36.8	16.7	1.48	OK	60.0	23.7	15.5	1.46	OK	36.9	24.0	1.9	1.23	1.2	0.211
C	45.0	40.0	12.6	1.37	Break						40.8	24.6	1.5	1.29	1.8	0.210
D	25.0	30.4	16.0	1.47	Crease	60.0	24.3	15.5	1.46	OK	30.6	24.0	3.7	1.01	1.0	0.148
D	50.0	35.6	16.3	1.47	OK	60.0	23.7	15.5	1.46	OK	35.8	24.0	2.1	1.20	2.1	0.153
D	60.0	38.1	15.8	1.47	Break						38.3	24.1	1.7	1.24	2.5	0.158

ardless of whether the lubricant exists in a dispersed manner in the coating film layer or in an enriched manner on the coating film surface. Furthermore, a simple method was devised for evaluating the coefficient of friction at die shoulder drawing under flange shrinkage deformation, which seems to be favorably responding to the above result.

### 2.3 Evaluation of coil characteristics developed in handling

#### 2.3.1 Method of evaluation of coil characteristics developed in handling

A study was conducted to evaluate the difference in coil characteristics developed in handling the developed coils and conventional coils by reproducing the actual state of coiled sheet slip and coil collapse, and capturing their behaviors. Two types of coils were evaluated: A, coated with the coating film containing surface-modified lubricant and B, coated with the coating film with lubricant without surface modification. These coils were produced by dividing a coil into two coils. The first half coil and the second half coil were provided with coating treatment A and B respectively. Accordingly, it can be considered that the specification (coil size, mechanical properties, and galvanized coating layer) of the substrate material other than the subject coating treatment is identical. Detail of the specification of the samples is shown in **Table 4**.

The coil reeling tension was changed using a recoiling line.

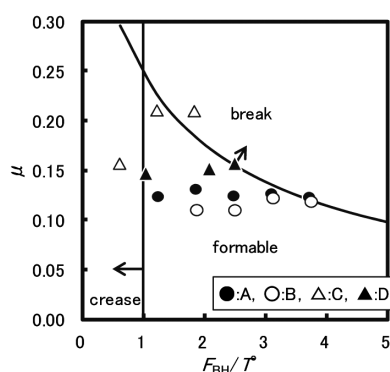


Fig. 5 Relations between the frictional coefficients and the blank hold conditions

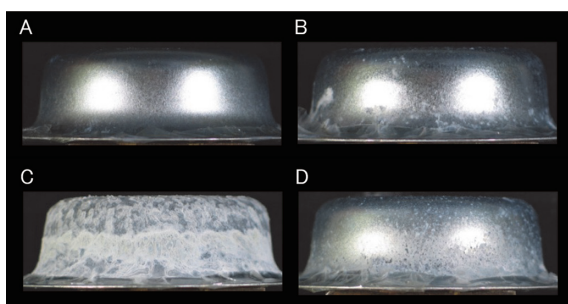


Photo 4 Appearance after SST 48h of the press forming works

**Photo 5** shows the pay-off reel in the state of completion of coiling. Evaluation was conducted in the following manner; as a mean to apply impact equal to the one actually applied at the time of unloading, the mandrel was shrunk (simulating the state of the coil being hooked), and then the coil car was moved upward (simulating the coil being placed on a flat place).

#### 2.3.2 Evaluation of coil collapse

After the application of the impact, the gap between the inner side of the coil and the sleeve was measured with a gap measuring gauge and the amount of deformation of coil internal circularity was evaluated with formula (5).

Deformation of coil internal circularity ( $\Delta d$ )

$$\equiv \text{horizontal diameter} - \text{vertical diameter} = (g_U + g_B) - (g_L + g_R) \quad (5)$$

where; sleeve/coil internal diameter gaps; upper/ $g_U$ , bottom/ $g_B$ , left/ $g_L$  and right/ $g_R$

**Figure 6** shows the relationship between the deformation of coil internal circularity (coil collapse) and reeling tension. The reeling tension that develops deformation of coil internal circularity is not different between A and B, and stays in the region of  $T < 20$  MPa. From this, it is found that the coefficient of friction is not the direct factor of the deformation of coil internal circularity but the factor that

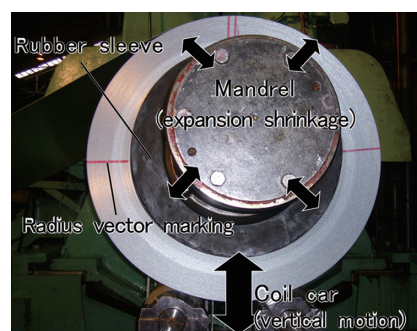


Photo 5 Method to impact on a coil  
It was applied with a payoff reel by the mandrel shrinkage and coil car up-and-down motion.

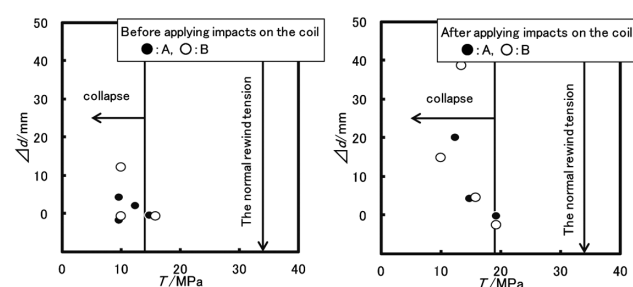


Fig. 6 Relations between coil collapse and the rewind tension  
Left: After the mandrel shrinkage, Right: Furthermore, hang it, and unload it (these impacts were applied)

Table 4 Details of test materials

Coating	Lubricant (included in coating)	Plating layer (finish of substrate)	Sheet thickness mm	Width mm	Steel class	Coil weight ton
A	Modified solid lubricant	Hot-dip galvanizing	0.6	1 220	Low carbon	10
B	Conventional solid lubricant	Same as A	Same as A	Same as A	Same as A	10



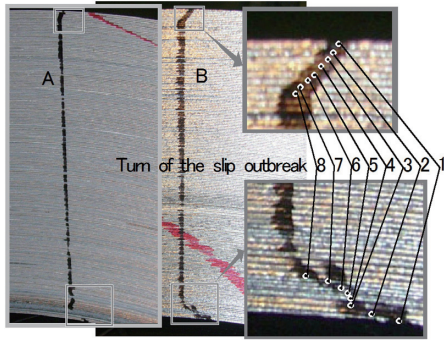


Photo 6 Slip gap that was caused by 8 times of impacts ( $T=19.2$  MPa)

governs the process of coil loosening leading to the deformation of coil internal circularity. Furthermore, in Fig. 6, the left figure shows the case without application of impacts and the right figure shows the case with application of impacts, respectively, and only the point where the possible deformation of coil internal circularity induced by impacts starts is observable and no significant difference is observed between A and B.

**Photo 6** shows the state of coiled sheet slip after the application of eight impacts. Since it is confirmed that in both A and B, coiled sheet slip from the original line marked in the radius vector direction is taking place at the eight coiled sheets on outer and inner sides of the coil after the application of eight impacts, it is found that slip at a coiled sheet takes place once per impact. In contrast, since slip of smaller amount as compared to B is observed on A, it is known that the amount of drop of tension per impact is smaller in A where coefficient of friction is higher.

As mentioned above, enhancing coefficient of friction makes the amount of drop of tension per slip smaller, and therefore, is effective as a countermeasure for improving coil characteristics developed in handling. What needs attention is that even if coefficient of friction is enhanced, the limit tension at which coil collapse begins to take place remains unchanged.

### 2.3.3 Analysis

Study on finding tension by measuring the change in strain due to coil sheet slip was conducted. Also calculation of coefficient of friction based on the tensions before and after coiled sheet slip was attempted.

To quantify the change in tension due to change in strain, a coil on which a straight line was marked in the radius vector direction was recoiled repeatedly with varied tensions and scaling was conducted for the relationship between tension and strain by tracking the movement of the straight line marking in the direction of radius vector. Change in strain was sought for with formula (6) through image analysis based on the coordinate as shown in **Photo 7**. **Figure 7** shows the relationship between tension and strain thus obtained. Approximate linearity was obtained in the relationship between tension and strain; however, the modulus of elasticity ( $E=15000$  MPa) which is the inclination of the straight line exhibited a small value of approximately one tenth of the generally known value of steel material. It is considered that the net material elongation strain is approximately 10% and the remaining 90% is caused by the change in filling ratio of gaps in a coil. Using this relation and by introducing the same coordinate as shown in **Photo 8**, tensions before and after slip caused by application of impacts can be sought for.

$$\Delta\sigma = \frac{t \cdot d\theta}{2\pi dr} = \frac{t \cdot \arccos \left[ \frac{(x_0 \cdot x_i + y_0 \cdot y_i)}{\{(x_0^2 + y_0^2)^{1/2} \cdot (x_i^2 + y_i^2)^{1/2}\}} \right]}{2\pi \{(x_0^2 + y_0^2)^{1/2} - (x_i^2 + y_i^2)^{1/2}\}} \quad (6)$$

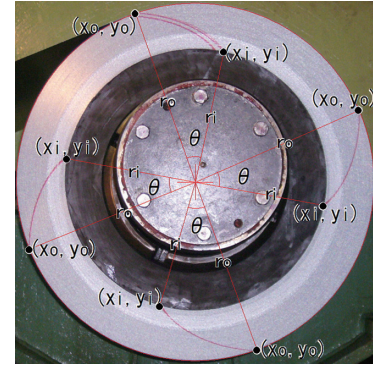


Photo 7 Image analysis coordinate of the radius vector marking that moved by tension reduction rewind

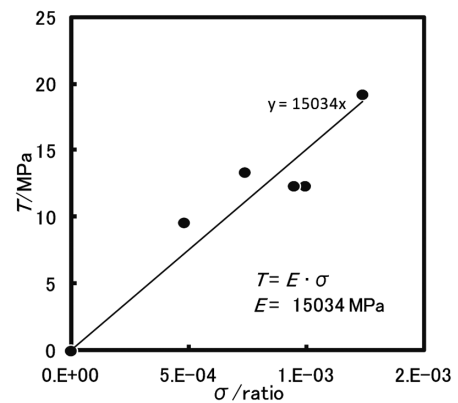


Fig. 7 Relations between rewinding tension and circumference strain

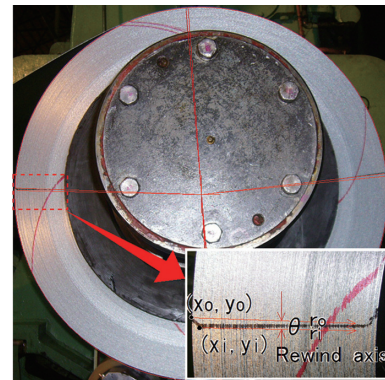


Photo 8 Movement of the radius vector marking (black mark) by slips and image analysis coordinate

**Figure 8** shows the coiled sheet slip propagation model to calculate coefficient of friction. This model is based on the concept that a slip comes to a halt when it comes to a point where the frictional force before relaxation and dragging tension during circumferential sliding becomes even, and expressed as equation (7).

$$T_{i0} = T_0 \cdot (e^{\mu\phi} - 1) = T + T_f = T \cdot e^{\mu\phi} \quad (7)$$

where dragging tension before coiled sheet slip

$$T_0 + T_{i0} = T_0 \cdot e^{\mu\phi} \quad (8)$$

dragging tension during slipping

$$T + T_f = T \cdot e^{\mu\phi} \quad (9)$$

$T_0$ : initial tension,  $T_{i0}$ : frictional force by initial tension,  $T$ : tension after relaxation (after slip),  $T_f$ : frictional force by tension

after relaxation,  $\phi$  : angle of winding

Solution of equation (7) for coefficient of friction leads to formula (10). However, since a slip takes place at one circumference sheet and then progresses one by one, it was assumed that winding angle is  $\phi = 2\pi$  and coefficient of friction  $= 2\mu$  as friction takes place on the front and back sides.

$$2\mu = \frac{1}{2\pi} \ln \left( \frac{T}{T_0 - T} \right) \quad (10)$$

**Table 5** shows the strain observed by changing the reeling tension at a recoiling line and the calculated values of tension and coefficient of friction obtained through backward calculation from the strain observed at the coil slip location. The coefficient of friction became 0.18 for A and 0.10 for B. It was verified on actual coils that the countermeasure of eliminating the enrichment of solid lubricant on the surface and dispersing it in the coating film instead was effective in improving coil characteristics developed in handling.

The change of tension within a coil caused by repetition of application of impact was simulated using the coefficient of friction and the modulus of elasticity thus obtained. **Table 6** shows the simulation condition.

**Figure 9** and **Fig. 10** show the result of the simulation, showing

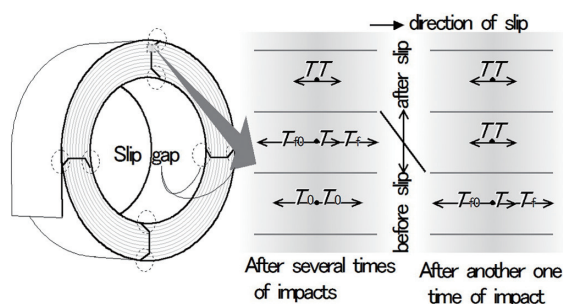


**Fig. 8** Model describes the tensile relaxation which depends on the friction

how radius vector marking is moving due to coiled sheet slip. The sphere of the tension under 20 MPa that develops coiled sheet slip is indicated with red line and the sphere of the tension where 20 MPa or above is retained is indicated with blue line. As opposed to B where the tension that triggers coil collapse is reached at inner and outer peripheral after 72 impacts, remarkable improvement was noticed in A with 360 impacts before collapse. As indices of coil characteristics developed in handling, coefficient of friction within a coil, tension retention ratio per slip, and the number of handling where coil collapse appears are tabulated (**Table 7**).

For coil transportation to outside of a mill, coils are bundled with strap after wrapping, and therefore, it is not mistakable that the coils are more or less in a favorable condition, more so than the condition where study was made, and it is considered that probably coil rigidity is increased and the fluctuation of tension within a coil becomes smaller, lowering the probability of the occurrence of coiled sheet slip due to impacts. The quantitative investigation that tracks how coils behave in actual delivery history with radius vector marking on actually mass-produced coils is a subject left for future study. Although authors realize that the problems relating to handling of slippery steel sheets have subsided owing to the efforts and devices of customers, it is also a factual matter that problems relating to coil handling have not been heard of since after this technology was put into practice.

#### 2.4 Compromise between press formability and coil characteristics developed in handling

Since provision of press formability and deterioration in sheet coil characteristics developed in handling are attributed to one single factor of solid lubrication material, they are contradictory in nature. **Figure 11** shows the relationship between the coefficient of friction under coil handling and the coefficient of friction under press forming with respect to A where solid lubricant is dispersed in coating film layer and to B where solid solution is enriched on surface layer. Although coefficients of A and B under press forming do not differ greatly, the coefficient of A under coil handling is much higher and

**Table 5** Result of the handling coil test and its analysis

Result of the handling coil test						Result of analysis				
Test No.	Sample	$\frac{T}{\text{MPa}}$	Impact	$\frac{\Delta d}{\text{mm}}$	Collapse judgement	Object domain	$\frac{L^*}{\text{m}}$	$\frac{N^*}{\text{number}}$	$\frac{T}{\text{MPa}}$	$\frac{\sigma}{\text{ratio}}$
1-1	B	10.0	Did not	12.4	NG					
1-2	B	15.8	Did not	-0.4	OK					
1-3	B	15.8	Applied	4.8	NG					
2-1	B	10.0	Did not	-0.4	OK					
2-2	B	10.0	Applied	15.1	NG					
2-3	B	13.4	Did not	-	OK				11.3	7.4E-4
2-4	B	13.4	Applied	38.9	NG					
2-5	B	19.2	Applied	-2.3	OK	Overall length	422.9	1 - 187	18.9	1.2E-3
	↑		↑	↑	↑	Sliped domain		179 - 187	14.8	9.7E-4
Mean properties of "B"										0.10
1-4	A	9.6	Did not	4.5	NG					
1-5	A	14.8	Did not	-0.2	OK					
1-6	A	14.8	Applied	4.5	NG					
2-6	A	9.6	Did not	-1.5	OK				7.4	4.8E-4
2-7	A		Applied	38.8	NG					
2-8	A	12.4	Did not	2.3	OK	Overall length	389.2	1 - 174	14.9 ± 0.4	9.7 ± 2E-5
2-9	A	12.4	Applied	20.3	NG	Sliped domain		170 - 174	13.5	8.9E-4
2-10	A	19.2	Applied	4.7	OK	Overall length	368.4	1 - 166	18.9	1.2E-3
	↑		↑	↑	↑	Sliped domain		160 - 166	16.9	1.1E-3
Mean properties of "A"										0.18 ± 0.03

\* L: Length of rewinding, N: Number of rewinding

Table 6 Simulation conditions of rewinding tension relaxation by applying repeating impacts

Item of conditions	Details of conditions																								
Specifications of model coils	<table><tr><th>Coating</th><th><math>\frac{t_s}{\text{mm}}</math></th><th><math>\frac{w_s}{\text{mm}}</math></th><th><math>\frac{m_c}{\text{ton}}</math></th><th><math>\frac{2r_0}{\text{inch}}</math></th><th><math>\frac{T_0}{\text{MPa}}</math></th><th><math>\frac{E}{\text{MPa}}</math></th><th><math>\mu</math></th></tr><tr><td>A</td><td>0.6</td><td>1000</td><td>10</td><td>20</td><td>34.4</td><td>15 034</td><td>0.18</td></tr><tr><td>B</td><td>↑</td><td>↑</td><td>↑</td><td>↑</td><td>↑</td><td>↑</td><td>0.10</td></tr></table>	Coating	$\frac{t_s}{\text{mm}}$	$\frac{w_s}{\text{mm}}$	$\frac{m_c}{\text{ton}}$	$\frac{2r_0}{\text{inch}}$	$\frac{T_0}{\text{MPa}}$	$\frac{E}{\text{MPa}}$	$\mu$	A	0.6	1000	10	20	34.4	15 034	0.18	B	↑	↑	↑	↑	↑	↑	0.10
	Coating	$\frac{t_s}{\text{mm}}$	$\frac{w_s}{\text{mm}}$	$\frac{m_c}{\text{ton}}$	$\frac{2r_0}{\text{inch}}$	$\frac{T_0}{\text{MPa}}$	$\frac{E}{\text{MPa}}$	$\mu$																	
	A	0.6	1000	10	20	34.4	15 034	0.18																	
B	↑	↑	↑	↑	↑	↑	0.10																		
	<p>* <math>t_s</math>: Sheet thickness, <math>w_s</math>: Sheet width, <math>m_c</math>: Mass of the coil, <math>2r_0</math>: Inside diameter of the coil, <math>T_0</math>: Initial tension, <math>E</math>: Elastic modulus (Fig. 6), <math>\mu</math>: Frictional coefficient (Table 5)</p>																								
Calculation	<p>Rewinded number (radius position) : <math>i = 1, 2, \dots, I</math> Repeated number of applied impacts : <math>j = 1, 2, \dots, J</math> Slip number after repeated impacts : <math>k_{ij} = \text{Integer}(J/I) + \text{If}(\text{Modulus}(J/I) \geq i, 1, 0)</math> Tension after repeated slips</p> $T_{ij} = \left( \frac{e^{4\pi\mu} - 1}{e^{4\pi\mu}} \right)^{k_{ij}} T_0$ <p>Phase angular position after repeated slips</p> $\theta_{ij} = 2\pi \sum_{i=1}^i \frac{T_0 - T_{ij}}{E}$ <p>Coordinate system to trace the slip gaps</p> $\begin{cases} x_{ij} = (r_0 + i \cdot t) \cdot \cos(\theta_{ij}) \\ y_{ij} = (r_0 + i \cdot t) \cdot \sin(\theta_{ij}) \end{cases}$ <p>Slip starting point: innermost peripheral and the outermost peripheral positions Biggest tension to coil collapse: 20 MPa</p>																								

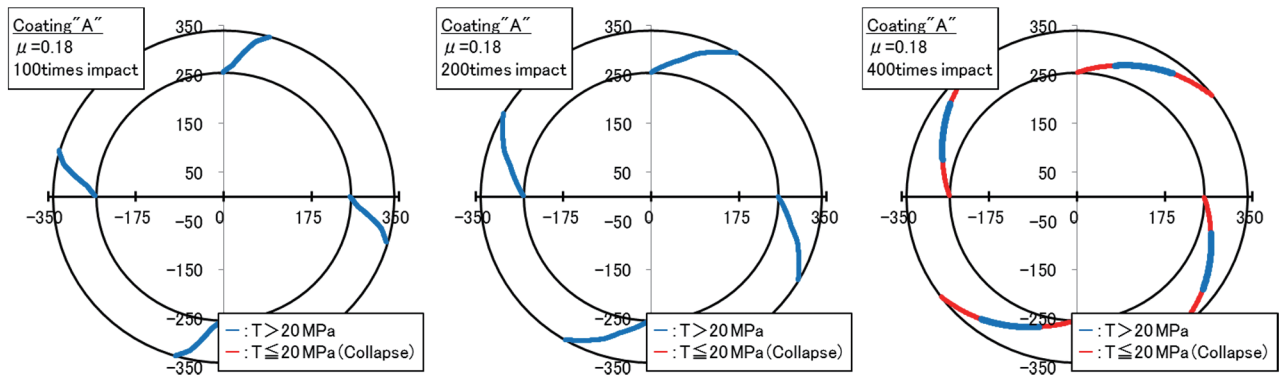


Fig. 9 Change of slip gap distribution on "A" after repeated impacts

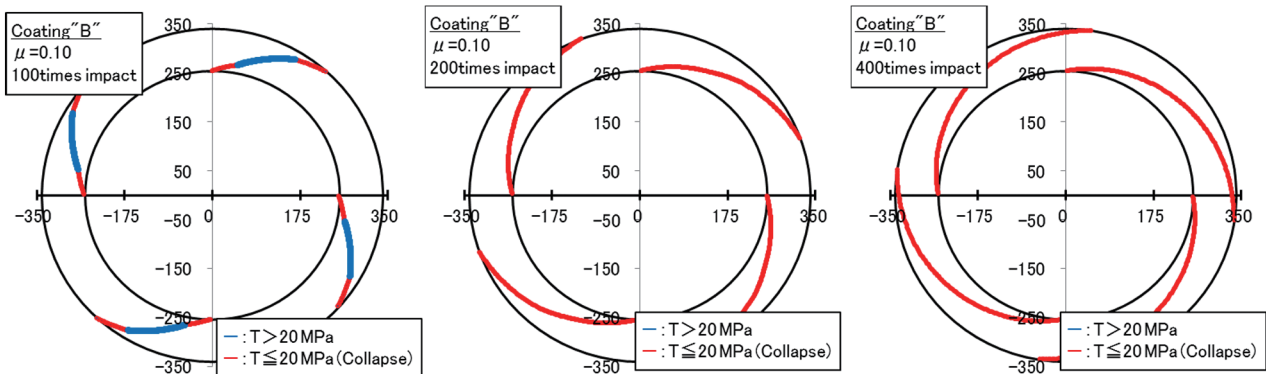


Fig. 10 Change of slip gap distribution on "B" after repeated impacts

Table 7 Index-value of handling a coil

Coating	Frictional coefficient	Tension retention by a slip	Number of repeating impact until coil collapse
A	0.18	81%	360
B	0.10	52%	72

improvement in compromise between the two performances is clearly noticed in A. Thus, concept of sliding conditions of press forming, coil transportation, and piling are outlined in the table, and as the conclusion, it is considered that under press forming, inside characteristics of the coating film layer, and under coil transportation and piling, surface characteristics of the coating film layer, are becoming governing factors respectively over sliding characteristics and could improve the compromising situation in favor of both the two performances which are contradictory in nature (Table 8).

## 2.5 Other performances

Evaluation of DURGRIP™ QS2 with respect to corrosion resistance, spot weld weldability and adhesion characteristics of overcoat painting was also conducted. Evaluation conditions are shown in Table 9.

Photo 9 shows the appearance of a sample after 72 h of SST. No

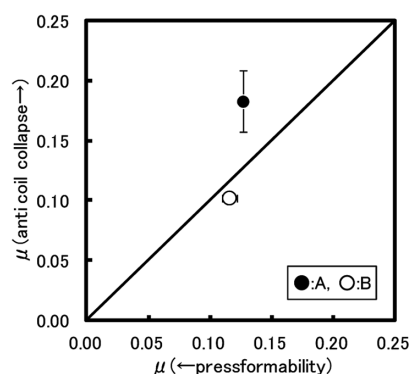


Fig. 11 Relations between two kinds of frictional coefficients, vertical axis relates to handling and the horizontal axis relates to forming

Table 8 Small consideration about the slide interface under press forming and under handling acoil or a sheet pile

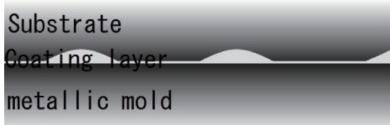

Item of consideration	Under press forming	Under handling acoil (or a sheet pile)
Aspect pressure	300 - MPa (plastic flow stress of substrate)	0.01 - 0.3 MPa (0 - 3 MPa)
Phenomenon of the load	Relaxation of the contact stress by substrate plastic flow (300 - MPa) 	Relaxation of the contact stress by the compression elasticity of the film layer (- 50MPa) 
Change of coating layer	Film squeezed out fills up the surface coarseness of substrate Film layer intervenes under the high aspect pressure that surpassed films plastic flow stress	Topological immutability
Sliding surface	Inside of the film layer	Surface of the film layer

Table 9 Method of evaluation test for the other compatibiliys

Item of evaluation	Detail of evaluation testing method
<u>Corrosion-resistance</u>	<u>Corrosion accelerating environment</u> : SST (JIS Z 2371) <u>Additional corrosion factor by the usages</u> 1. Bulging: Ericksen method at 7 mm high (added to the half bottoms of the test peace) 2. Scratch wound: Cross cut reaches the steel substrate (added to the half bottoms of the test peace) 3. Cutted endface: Protection with the polyester tape seal <u>Evaluation</u> : Corrosion appearance after SST 72 h continuation
<u>Spot weldability</u>	<u>Spot welder specification</u> Welder: "C" type Electrode tip specifications: DR type16 × 6 (40R), Material: Chromium-copper alloy <u>Welding condition</u> Welding power supply: AC 200 V/60 Hz Load: 2 kN, Cooling water flow: 2 L · min <sup>-1</sup> Electricity schedule: Squeeze / 5 cycle and electricity / 10 cycle and hold / 1 cycle Running in welding: 50 times with cold rolled steel sheet at the current of 6 kA Conditions of electricity: 5 - 15 kA (until fusion-bonding of tip with material, at suitable distances) <u>Measurement</u> : Break strength and nugget diameter of the shear specimen by the spot welding <u>Evaluation</u> : 1. Nugget formation electric current (nugget diameter ( $D_n$ ) of the $4\sqrt{t}$ equivalency) 2. Spark outbreak electric current 3. Fusion-bonding outbreak electric current 5. Appropriate current range between nugget formation and spark outbreak
<u>Compatibility as a painting sustrate</u>	<u>Orver coat painting</u> Paint: Melamine-alkyd resin coating (GLIMIN #500 WHITE product of SHINTO PAINT CO., LTD.) Orvercoat thickness: 25 μm, curing condition: 120°C × 25 min <u>Evaluatin</u> Adhesion with over coat: Cross cut test (10 × 10) Primary test: As painted sheet Waterproof test: After immersion in boiling water for 1 h



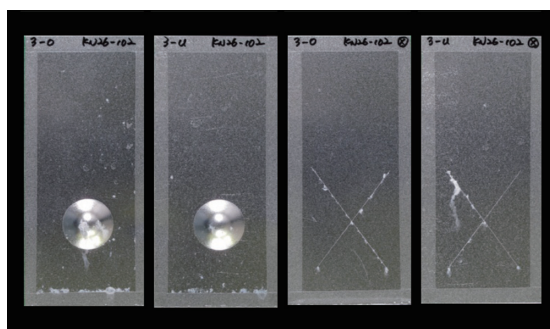


Photo 9 Appearance of test piece after SST 72 h

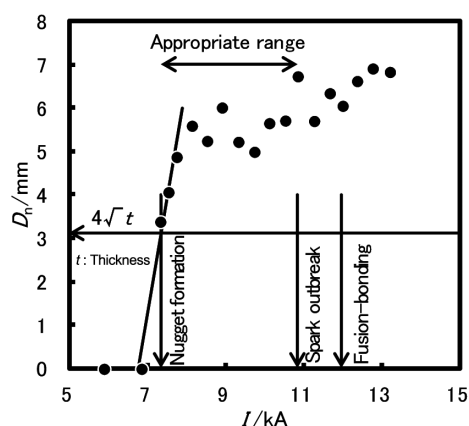


Fig. 12 Nugget diameter and welding phenomena with the variety of electric currents

white rust exceeding 5% is noticed on the flat part and even on worked out part and scratched part, generation of white rust is suppressed and good corrosion resistance is exhibited.

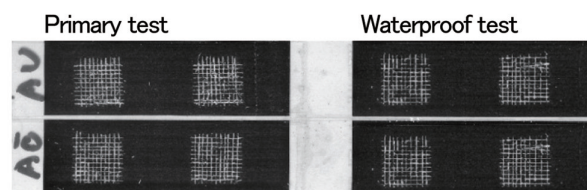


Photo 10 Appearance of peeled tapes after cross cut test

Figure 12 shows the relationship between spot welding nugget diameter and welding current. Appropriate current range between nugget forming current and dust generating is sufficiently available and possibility of spot welding was also confirmed.

Photo 10 shows the appearance of peeled tapes after overcoat paint adhesion test. Good primary adhesion and waterproof secondary adhesion were obtained.

### 3. Conclusion

As mentioned above, DURGRIP™ QS2 is a hot dip galvanized steel sheet with enhanced universality, provided with high adaptability to wide range of sheet metal processing conducted by steel sheet users, characterized by ① corrosion resistance, ② lubricity, ③ spot weld weldability, and ④ adhesion characteristics of overcoat painting. In particular, countermeasures were taken for problems caused by coil characteristics developed in handling such as coil collapse and break of pile of coils due to slip, a side effect of providing lubricity, and high compatibility with non-oiling press formability was attained simultaneously.

Authors will continue research and development to further pursue ease of use.

### References

- 1) Matsuda, T., Kubota, T.: GALVATECH'07. 2007, p. 745-750
- 2) Takahashi, S., Yoshida, K., Ikishima, K.: CAMP-ISIJ. 9, 1426 (1996)



Ken TOMIYASU  
Senior Manager  
Steel Sheet Products Development Dept.  
Quality Management Div.  
Kashima Works  
3 Hikari, Kashima City, Ibaraki Pref. 314-0014



Hiroki TAKAMARU  
Manager  
Steel Sheet making technology Dept.  
Sheet & Coil Div.  
Wakayama Works



Yasuo TSUJIMOTO  
Manager  
Steel Sheet making technology Dept.  
Sheet & Coil Div.  
Wakayama Works



Eiji MAEDA  
Foreman  
Galvanizing Steel Sheet Making Plant  
Sheet & Coil Div.  
Wakayama Works